

## Nonlinear Spectroscopy of Cold Atoms in a Spontaneous-Force Optical Trap

J. W. R. Tabosa,<sup>(a)</sup> G. Chen, Z. Hu, R. B. Lee, and H. J. Kimble

*Norman Bridge Laboratory of Physics 12-33, California Institute of Technology, Pasadena, California 91125*

(Received 5 December 1990)

Probe-wave amplification and absorption spectra are reported for cesium atoms cooled and confined in a Zeeman-shift spontaneous-force optical trap. Novel spectral features are observed with narrow frequency widths and with single-pass gain of 20% in some cases. Negative radiation pressure is demonstrated as the mechanical consequence of optical gain and is investigated as a possible means for optical implosion of a trapped sample.

PACS numbers: 32.80.Pj, 32.70.-n, 42.50.Vk, 42.65.Ft

The past several years have witnessed a phenomenal pace of achievement in the field of laser cooling and trapping of atoms,<sup>1</sup> with the powerful techniques that have been developed now finding a variety of scientific applications. Of particular interest from the perspective of laser spectroscopy are the capabilities for producing optically dense samples of cold atoms with number densities greater than  $10^8/\text{cm}^3$  and temperatures below 100  $\mu\text{K}$ .<sup>1-5</sup> The opportunities for spectroscopic investigations in this domain are quite exciting since the role of a number of complications (including Doppler and transit broadening) can be greatly reduced. Moreover, detailed spectroscopic characterizations can provide important new information about the dynamics of the trap itself and can suggest new avenues for improved trapping and cooling.

Motivated by these considerations, in this Letter we report measurements of the spectral response of a collection of laser-cooled and -confined cesium atoms to a weak probe beam in the presence of strong saturating beams that form an optical trap. Over a range of trapping parameters, we record transmission spectra for the probe beam and observe regions of both large absorption and gain. Certain broad features of the absorption spectra are in reasonable agreement with earlier work for two-state atoms in a strong field.<sup>6</sup> However, narrow spectral features are observed around the frequency of the trapping beams with widths well below the natural radiative linewidth and with large single-pass gain. We explore the correlation between these narrow spectral resonances and the morphology of the trap and in particular observe both positive and negative radiation pressure associated with stimulated absorption and emission from the probe beam. Contrary to the normal circumstance of a repulsive interaction, we suggest that negative radiation pressure can give rise to a long-range attractive force which might be employed for optical implosion of a trapped sample.

Our experiments employ atomic cesium in a Zeeman-shift spontaneous-force optical trap<sup>2-5</sup> (ZOT) as illustrated in Fig. 1. The trap is similar in concept to that originally demonstrated by Raab *et al.*<sup>2</sup> but with the important distinction that it is loaded directly from cesium vapor in a quartz cell.<sup>3</sup> A dissipative cooling force is

provided by three counterpropagating pairs of laser beams of opposite circular polarization arranged along mutually orthogonal directions and with common frequency tuned several natural linewidths below the resonant transition ( $6S_{1/2}, F=4 \rightarrow 6P_{3/2}, F'=5$  at 852 nm). A spatially dependent trapping force arises from the position dependence of the atomic Zeeman shift in an inhomogeneous magnetic field of gradient of 10 G/cm along  $z$  and 5 G/cm along  $(x, y)$  created by two current carrying coils.<sup>2</sup> In steady state, the number of trapped atoms is determined by the balance of laser capture from and collisional loss with the background of Cs vapor in the cell.<sup>3</sup> The typical filling time of the trap following a sudden turn-on of the trapping lasers is about 1 s for a cell with Cs pressure  $2 \times 10^{-8}$  Torr, with the diameter of the steady-state cloud of trapped Cs atoms being about 1 mm. The temperature of the trapped atoms is near the Doppler cooling limit<sup>3-5</sup> as inferred by monitoring the decay in absorption of a weak probe beam when the trapping lasers are chopped off. In our experiments, the trapping beams are of waist  $w_0=4$  mm and are derived from a frequency-stabilized Ti:Al<sub>2</sub>O<sub>3</sub> laser with linewidth below 100 kHz. Radiation from a semiconductor-diode laser recirculates population lost to the  $F=3$  ground state.

Given this brief survey of the ZOT, we next turn to our spectroscopic study to investigate more explicitly the

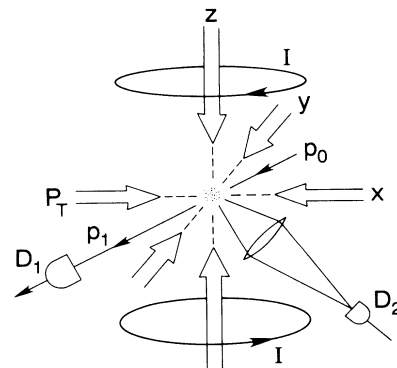


FIG. 1. Diagram of Zeeman-shift spontaneous-force optical trap (ZOT).

microscope dynamics of the trap. Again with reference to Fig. 1, under conditions of strong excitation by the trapping lasers, we record transmitted power as a function of frequency  $\omega_p$  for a low-intensity probe beam of waist  $\approx 100 \mu\text{m}$  focused through the trap. The probe beam is derived from the Ti:Al<sub>2</sub>O<sub>3</sub> laser and is independently tuned over a limited range in frequency by acousto-optic modulators. Figure 2 is typical of our results for the probe spectra and is a succession of records of the transmitted probe power normalized to the input probe power ( $p_1/p_0$ ) vs  $\omega_p$ , with the positions of the frequencies of the trapping laser  $\omega_T$  and of the atomic transition  $\omega_A$  indicated. As might be expected,<sup>6</sup> we observe in Figs. 2(a) and 2(b) probe spectra with broad regions of absorption and amplification symmetrically placed about  $\omega_T$  characteristic of the dressed-state splitting. However, in addition to the broad features, a narrow dispersive-shaped feature around  $\omega_T$  is also clearly evident in Figs. 2(a) and 2(b). This narrow feature has a

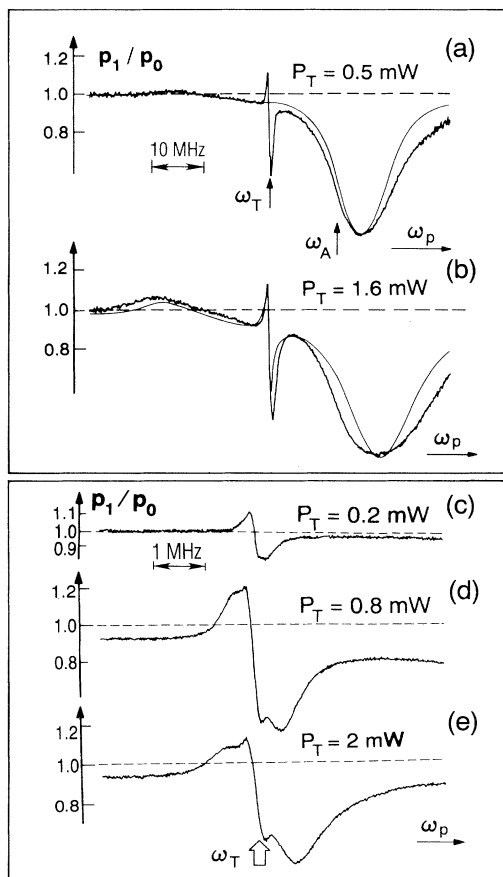


FIG. 2. Probe absorption spectra  $p_1/p_0$  vs probe frequency  $\omega_p$  for  $(\omega_A - \omega_T)/2\pi = 13.5$  MHz. (a), (b) Scans showing large absorption near  $\omega_A$  and small gain symmetrically placed about  $\omega_T$ . (c)–(e) Magnified frequency scale to examine the narrow central feature near  $\omega_T$  for various  $P_T$ . The finely drawn curves in (a) and (b) are discussed in the text.

width below the natural linewidth of  $\gamma_{\perp}/\pi = 5$  MHz and can exhibit appreciable single-pass gain ( $> 20\%$ ). An expanded view of the absorption spectrum is given in Figs. 2(c)–2(e), where we see that for increasing levels of trapping power  $P_T$ , the dispersive shape broadens and develops substructure. The general trends shown in Fig. 2 are independent of the number of trapped atoms as well as of the direction of propagation of the probe beam relative to the trapping beams. However, the spectra do exhibit a dependence on the polarization state of the incident probe beam [especially as regards the substructure shown in Figs. 2(c)–2(e)] and on the magnetic-field gradient across the trap ( $\Delta B \sim 1$  G gives a range  $\Delta\omega_A/2\pi \sim 1$  MHz).

To model these probe spectra, we can make some headway by first of all attempting to assess the role of the multiplicity of Zeeman transitions with a crude adaption of the standard two-state result.<sup>6</sup> Our approach is to average absorption spectra for a weak probe over the distribution of dipole moments for the  $F=4 \rightarrow F'=5$  transition in Cs. As indicated by the finely drawn curve in Fig. 2(a), the agreement between this calculation and the experiment is qualitatively reasonable exclusive of the narrow feature. Pursuing this analysis somewhat further, we present in Fig. 3 a compilation of results such as in Fig. 2(a) over a range of trapping power  $0 \leq P_T \leq 3$  mW. With regard to the splitting  $\tilde{\Omega}$  between  $\omega_T$  and the broad absorption feature, we find that the average over Zeeman sublevels does not produce significant departures from the two-state result. By contrast, the large spread in Clebsch-Gordan coefficients within the  $F=4 \rightarrow F'=5$  manifold results in a broadening that substantially increases the width  $\beta$  above the two-state result for both the experimental scans and the calculation. That this excess width does not arise from heating of the trap with increasing

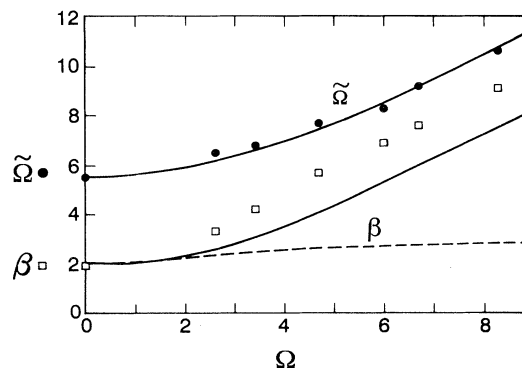


FIG. 3. Frequency splitting  $\tilde{\Omega}$  (●) and width  $\beta$  (□) of the broad absorption feature vs Rabi frequency  $\Omega$  of trapping beams for  $(\omega_A - \omega_T)/2\pi = 13.5$  MHz. Theoretical curves for  $\tilde{\Omega}$  and  $\beta$  are from an average for  $F=4 \rightarrow F'=5$ . The dashed curve gives  $\beta$  for the single two-state transition; a similar curve for  $\tilde{\Omega}$  would roughly overlay the multistate result. The normalization for  $\tilde{\Omega}$  and  $\beta$  is  $\gamma_{\perp}/2\pi = 2.5$  MHz; for  $\Omega$  it is  $\sqrt{2}\gamma_{\perp}$ .

$P_T$  has been established with measurements both of the transient decay of the trap and of the probe spectrum with a chopping technique that leads to the points for  $(\Omega, \beta)$  at  $\Omega=0$ . Note that in Fig. 3,  $\Omega$  is referenced to the  $m_F=4 \rightarrow m_F=5$  transition with  $\Omega=1$  for  $I=1$  mW/cm<sup>2</sup>, where  $I=6I_T$  and  $I_T=2P_T/\pi\omega_0^2$ . The set of theoretical Rabi frequencies has been scaled by  $a=0.85$  ( $\Omega \rightarrow a\Omega$ ) to optimize the comparison.

If we next consider the narrow central feature near  $\omega_T$ , we might attempt to account for the rather complex optical pumping processes within the manifold of Zeeman states with an extension of the usual two-state calculation to include relaxation to and from neighboring Zeeman transitions. As opposed to our previous summation, such an approach for an "open" two-state system offers the possibility for describing certain dynamical aspects of the problem, as for example, the differential rate of relaxation of ground- and excited-state populations.<sup>7,8</sup> Unfortunately, the spectrum for the open two-state system exhibits either very small central features of the same symmetry as in Figs. 2 or larger features of size comparable to our data but of opposite symmetry.<sup>7</sup> Fortunately, a generalization of the open two-state model to multistate systems that do not conserve alignment or orientation finds the possibility for reversals in sign of narrow resonances.<sup>8(a)</sup> If we follow this lead and make an otherwise *ad hoc* change of sign in the terms responsible for the narrow feature (Eq. 4 of Ref. 7), we obtain surprisingly good agreement between the resulting analytic expression and our spectra as evidenced by the comparison in Fig. 2(b), for which the external decay rates of the ground and excited states are  $\nu_1/\gamma_\perp=0.4$  and  $\nu_2/\gamma_\perp=1.2$ . Although this circumstance might simply be a curiosity, recent theoretical work<sup>8(b)</sup> may provide an acceptable justification for what is otherwise simply a fitting function. Independent of this, another avenue that we have followed is to calculate absorption spectra for a three-level  $\Lambda$  scheme for which slow relaxation between ground states can lead to narrow spectral features.<sup>9</sup> For weak excitation, narrow Raman resonances appear at  $\omega_T \pm \delta$  in the probe spectra, with  $\delta$  as the frequency splitting of the ground states. For appropriate choices of decay rates and Rabi frequencies, spectra with features qualitatively similar to those in Fig. 2 can be obtained. Presumably the differential detuning  $\delta$  in this calculation reflects the range of Doppler shifts and spatially dependent Zeeman splittings across the trap, while the mixing of ground states is driven by atomic motion through the polarization gradients of the trap. Although this model is encouraging for weak fields, unfortunately for strong excitation as in Figs. 2 and 3, the calculated absorption spectra depart significantly from our traces as the field-dependent dressed states for the  $\Lambda$ -system emerge.

The decidedly mixed scorecard for the above analyses leads us to conclude that a detailed understanding of the absorption spectra will likely require a complex treat-

ment of the relevant cesium levels together with the microscopic environment of the trap. Not surprisingly then, our measurements of absorption spectra bring us full circle back to the difficult question of the self-consistent relationship between the spectroscopic and mechanical characteristics of the trap. To begin to address this issue, we present in Fig. 4 a series of images that illustrate a correlation between the narrow spectral resonances and the morphology of the trap. Figure 4(a) is a relatively symmetric picture of the trapped cloud of Cs atoms in the absence of the probe beam. In Fig. 4(b) the probe beam is present and is tuned for absorption in the narrow feature in Fig. 2. In this case the atoms in the trap recoil along the direction of propagation of the probe beam (stimulated absorption resulting in positive radiation pressure). In Fig. 4(c) the probe frequency is tuned into the region of gain in the subnatural profile, with the result that the atoms in the trap recoil opposite to the direction of propagation of the probe beam (stimulated emission resulting in "negative" radiation pressure).<sup>10</sup> Among the various applications that these images suggest, one is a technique for measuring the trap parameters based upon modulation of the probe  $p_0$  at frequency  $\nu$  while an image of the trap is monitored in fluorescence  $S$  with a split photodetector  $D_2$ , resulting in the (spatially resolved) trap transfer function  $S(\nu)/p_0(\nu)$ . (This open-loop response could even be "closed" for active servo control of the trap.)

Beyond the discussion for our particular trapping configuration, the images in Fig. 4 together with more general calculations of absorption spectra also suggest new mechanisms for dramatically altering the trap itself.

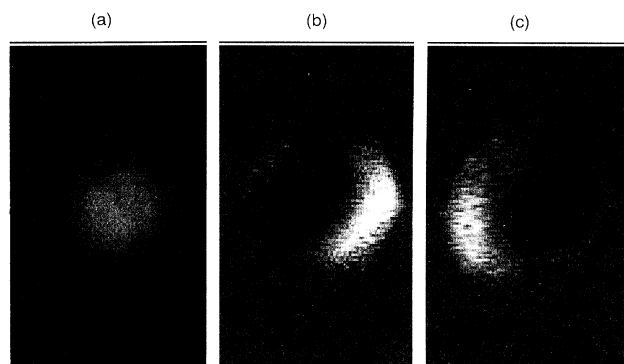


FIG. 4. Images of trapped cesium atoms viewed from  $[1\bar{1}0]$  direction (Fig. 1). (a) Trap in the absence of the probe beam with radius  $R \sim 0.4$  mm. (b), (c) Trap with probe beam propagating from left to right and into the page by about  $25^\circ$  (along  $[130]$  direction). (b) Probe detuning  $(\omega_p - \omega_T)/2\pi \approx +0.3$  MHz, with recoil along the direction of probe propagation (absorption). (c) Probe detuning  $(\omega_p - \omega_T)/2\pi \approx -0.3$  MHz, with recoil opposite to the direction of probe propagation (gain). In (b) and (c), the images shown are the difference between (a) and the corresponding image in the presence of the probe beam, with light (dark) indicating an increase (decrease) in atomic fluorescence.

For example, in an optically dense sample conventional radiation pressure leads to a long-range repulsive force between atoms [recoil away from the radiation source as in Fig. 4(b)].<sup>11</sup> If, however, the absorption cross section for scattered photons could be made negative, then a long-range attractive force between atoms would arise [recoil toward the radiation source as in Fig. 4(c)]. While in Fig. 2 the absorption cross section  $\sigma(\omega)$  is evidently negative (gain) only over small frequency intervals, recent work has described the possibility of probe gain over the entire frequency range of the atomic response.<sup>12</sup> Motivated by Refs. 11 and 12 we have attempted to identify in our calculations of probe spectra an operating regime which is spectroscopically suitable for the operation of the ZOT and which also gives a large frequency interval with  $\sigma(\omega) < 0$ . One of several possibilities is documented in Fig. 5, where we plot the frequency-resolved absorption cross sections for the  $V$  transition shown in the inset. Note that for the conditions defined in the caption, the  $1 \leftrightarrow 2$  transition is inverted and the fluorescence from this transition dominates that of the  $1 \leftrightarrow 3$  transition both as regards the rate of spontaneous emission (population of 2 greater than population 3 and  $\gamma_3 > \gamma_1$ ) and as regards the magnitude of the absorption cross section ( $|\sigma_{12}| \gg |\sigma_{13}|$ ). Hence the accompanying negative radiation pressure [ $\sigma_{12}(\omega) < 0$ ] in a dense sample should lead to an attractive force which might be employed for optical implosion of the sample.<sup>13,14</sup> Also note that the ZOT associated with the levels in Fig. 5 could operate predominantly by stimulated absorption on the  $1 \rightarrow 3$  transition and stimulated emission on the  $2 \rightarrow 1$  transition, with a reduced role for spontaneous emission on these transitions and consequently with the potential for reduced temperature (the  $3 \rightarrow 2$  transition might proceed by superfluorescent emission of small  $\hbar k$  through intermediate levels). Similar considerations apply from our analyses of  $\Lambda$  and ladder systems indicating the generality of these ideas. Detailed calculations including the integration of  $\sigma$  with the relevant emission spectra have been made and will be reported separately.

In conclusion, we have described an investigation of the nonlinear spectroscopy of cesium atoms cooled and confined in a spontaneous-force optical trap and have illustrated the mechanical effect of optical gain. We have also suggested the possibility of more dramatic manifestations of negative radiation pressure, including optical implosion and trapping by way of stimulated processes. However, independent of a specific proposal, it should be clear that clouds of cold, trapped atoms offer exciting prospects for many spectroscopic investigations. For example, we are currently attempting to employ the gain in the probe spectrum to achieve lasing in this novel system.

This work was supported by the National Science Foundation, by Venture Research International, by the Office of Naval Research, and by Conselho Nacional de Pesquisa-Brasil (J.W.R.T.). We are grateful to Profes-

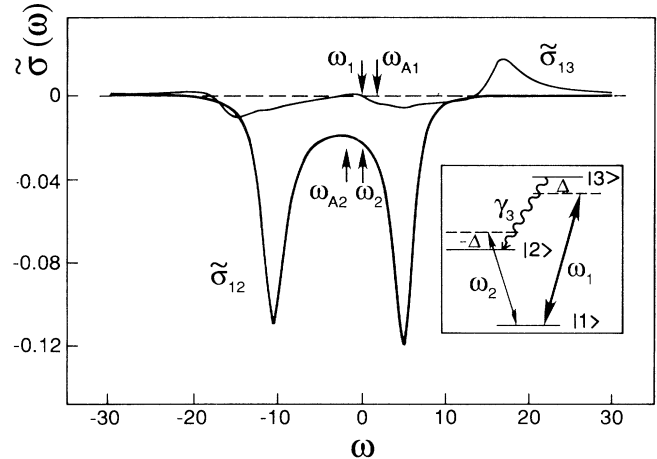


FIG. 5. Absorption cross sections ( $\tilde{\sigma}_{13}, \tilde{\sigma}_{12}$ ) vs frequency  $\omega$  near the  $1 \leftrightarrow 3$  ( $\omega_{A1}$ ) and  $1 \leftrightarrow 2$  ( $\omega_{A2}$ ) transitions. Strong saturating fields at  $\omega_1, \omega_2$  have Rabi frequencies  $\Omega_1 = 8, \Omega_2 = 1$  and are symmetrically detuned by  $\Delta = \pm 2$  as shown. The decay rates for  $3 \rightarrow 1$  and  $2 \rightarrow 1$  are  $\gamma_1 = \gamma_2 = 0.5$ , while  $\gamma_3 = 1.5$ .  $\tilde{\sigma}$  is normalized to  $\sigma_0 = (3/2\pi)\lambda^2$  for each transition.

sor C. Wieman and Professor T. Walker whose generosity helped to initiate this program and to Professor K. Libbrecht for important contributions.

*Note added.*—Since this work was submitted, spectra similar to those in Fig. 2 have been reported by Grison *et al.*<sup>15</sup>

(a)Permanent address: Departamento de Fisica, Universidade Federal de Pernambuco 50739 Recife, PE, Brazil.

<sup>1</sup>Laser Cooling and Trapping of Atoms, edited by S. Chu and C. Wieman [J. Opt. Soc. Am. B **6**, 2020–2278 (1989)].

<sup>2</sup>E. L. Raab *et al.*, Phys. Rev. Lett. **59**, 2631 (1987).

<sup>3</sup>C. Monroe *et al.*, Phys. Rev. Lett. **65**, 1571 (1990).

<sup>4</sup>A. M. Steane and C. J. Foot, Europhys. Lett. **14**, 231 (1991).

<sup>5</sup>A. Cable, M. Prentiss, and N. P. Bigelow, Opt. Lett. **15**, 507 (1990).

<sup>6</sup>B. R. Mollow, Phys. Rev. A **5**, 2217 (1972); S. Haroche and F. Hartmann, Phys. Rev. A **6**, 1280 (1972); F. Y. Wu *et al.*, Phys. Rev. Lett. **38**, 1077 (1977).

<sup>7</sup>A. D. Wilson-Gordon and H. Friedmann, Opt. Lett. **14**, 390 (1989).

<sup>8</sup>(a) P. R. Berman *et al.*, Phys. Rev. A **38**, 252 (1988); (b) P. R. Berman, Phys. Rev. A **43**, 1470 (1991).

<sup>9</sup>V. S. Letokhov and V. P. Chebotayev, *Nonlinear Laser Spectroscopy* (Springer-Verlag, Berlin, 1977), Chap. 5.

<sup>10</sup>The probe intensity  $I_p$  for Fig. 4 is about 4 mW/cm<sup>2</sup>, while Fig. 2 is taken with  $I_p$  below 0.4 mW/cm<sup>2</sup> so that the spectra are independent of probe power and do not exhibit such large recoil.

<sup>11</sup>D. W. Sesko *et al.*, J. Opt. Soc. Am. B (to be published).

<sup>12</sup>L. M. Narducci *et al.*, Phys. Rev. A **42**, 1630 (1990).

<sup>13</sup>Independent experiments to investigate such phenomena are in progress [C. Wieman (private communication)].

<sup>14</sup>J. Dalibard, Opt. Commun. **68**, 203 (1988).

<sup>15</sup>D. Grison *et al.*, Europhys. Lett. (to be published).

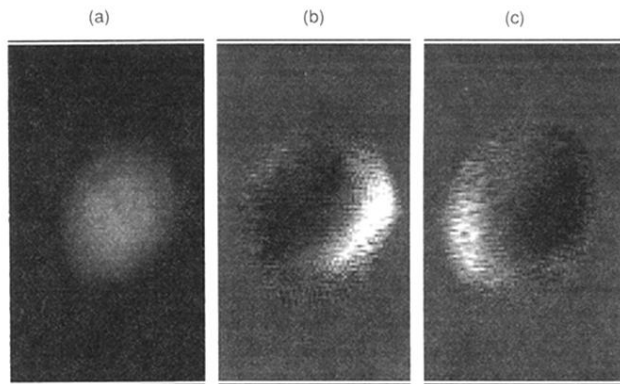


FIG. 4. Images of trapped cesium atoms viewed from  $[1\bar{1}0]$  direction (Fig. 1). (a) Trap in the absence of the probe beam with radius  $R \sim 0.4$  mm. (b),(c) Trap with probe beam propagating from left to right and into the page by about  $25^\circ$  (along  $[130]$  direction). (b) Probe detuning  $(\omega_p - \omega_T)/2\pi \approx +0.3$  MHz, with recoil along the direction of probe propagation (absorption). (c) Probe detuning  $(\omega_p - \omega_T)/2\pi \approx -0.3$  MHz, with recoil opposite to the direction of probe propagation (gain). In (b) and (c), the images shown are the difference between (a) and the corresponding image in the presence of the probe beam, with light (dark) indicating an increase (decrease) in atomic fluorescence.